# 2D Transducer Array for High-Speed 3D Imaging System N. Okada*, M. Sato, HONDA ELECTRONICS CO., LTD., Aichi, Japan; C. Ishihara, AKISHIMA LABORATORIES (MITSUI ZOSEN) INC. Tokyo, Japan; Y. Tamura, Yamagata University, Yamagata, Japan


## Abstract

3D imaging system was developed utilizing a combination of sparse 2D arrays, the synthetic aperture focusing technique, and coded excitation of a solution for high-speed 3D ultrasound imaging, since it could formulate multiple transmitting beams as well as receiving beams with a minimum number of transmissions. A 40 × 40 array of PZT elements was fabricated with a conventional dice-and-fill process (each element: 2MHz, 1mm × 1mm). 3D images were successfully obtained for the standard ultrasound phantoms with 32 transmitters and 128 receivers. It is shown that the combination of the 2D array and the coded wavefront method is applicable in medical diagnosis.


## 1. Introduction

The internal structure of the human body is inherently three-dimensional, and is constantly in motion. Therefore, high speed three-dimensional (3D) diagnostic imaging systems are required for many medical stages from early diagnosis to surgical operations. The conventional diagnostic ultrasound imaging system, however, visualizes only a small cross section of an entire organ at a time, although it is a low-cost and safe diagnostic tool.

Recently, 3D ultrasound imaging systems have become available against the background of the development of high-speed computer systems. Some systems utilize a combination of mechanical and conventional electronic scans. However, a slow data acquisition rate limits the application range of these systems. Although the combination of a two-dimensional (2D) transducer array and electrical beam-forming provides faster 2D beam steering[1)], the need to repeat pulse transmission in multiple directions lowers the frame rate of the imaging process. Furthermore, the image quality is restricted by the transmitting beam being focused at fixed positions.

2D array transducers are attracting major interest for application to volumetric imaging in real time. Smith *et al.* described 2D array transducers with up to 6400 elements operating at frequencies between 2.5 and 5.0 MHz for real-time volumetric imaging[2, 3)].

We have proposed the adoption of the synthetic aperture focusing technique with Walsh function modulated ultrasound pulses[4)]. The system drives all the transmitters simultaneously with modulated waveforms. An advantage of such code-divided transmission over the time-divided one[5)] is a higher S/N and higher efficiency of data acquisition. Both the transmitting and receiving beams are synthesized using received echo waveforms obtained with a single transmission. The first system was developed for application to underwater 3D sonar[6)]. Then, we initiated a project to realize a high speed 3D ultrasound echography system which would enable us to observe the dynamical structures of the human body.

# Report Documentation Page

*Form Approved*
*OMB No. 0704-0188*



| 1. REPORT DATE | 2. REPORT TYPE | 3. DATES COVERED |
|---|---|---|
| **00 JUN 2003** | **N/A** | **-** |

| 4. TITLE AND SUBTITLE | 5a. CONTRACT NUMBER |
|---|---|
| **2D Transducer Array for High-Speed 3D Imaging System** | 5b. GRANT NUMBER |
| | 5c. PROGRAM ELEMENT NUMBER |
| 6. AUTHOR(S) | 5d. PROJECT NUMBER |
| | 5e. TASK NUMBER |
| | 5f. WORK UNIT NUMBER |
| 7. PERFORMING ORGANIZATION NAME(S) AND ADDRESS(ES) **Honda Electronics Co., Ltd., Aichi, Japan; Akishima Laboratories (MITSUI ZOSEN) INC. Tokyo, Japan;** | 8. PERFORMING ORGANIZATION REPORT NUMBER |
| 9. SPONSORING/MONITORING AGENCY NAME(S) AND ADDRESS(ES) | 10. SPONSOR/MONITOR'S ACRONYM(S) |
| | 11. SPONSOR/MONITOR'S REPORT NUMBER(S) |

12. DISTRIBUTION/AVAILABILITY STATEMENT
**Approved for public release, distribution unlimited**

13. SUPPLEMENTARY NOTES
**See also ADM001697, ARO-44924.1-EG-CF, International Conference on Intelligent Materials (5th) (Smart Systems & Nanotechnology)., The original document contains color images.**

14. ABSTRACT

15. SUBJECT TERMS

| 16. SECURITY CLASSIFICATION OF: | | | 17. LIMITATION OF ABSTRACT | 18. NUMBER OF PAGES | 19a. NAME OF RESPONSIBLE PERSON |
|---|---|---|---|---|---|
| a. REPORT | b. ABSTRACT | c. THIS PAGE | | | |
| **unclassified** | **unclassified** | **unclassified** | **UU** | **8** | |

## 2. Principle

In this section, we briefly describe the principle of the imaging system[4]. Ultrasonic waves are simultaneously transmitted from $N_T$ $(= 2^k)$ transmitters, and reflected echo waveforms are detected by $N_R$ receivers. We use sinusoidal waves of frequency $f_0$ modulated by a system of Walsh functions synchronized with a clock signal. The period of the clock signal, $\Delta t$, is equal to an integral multiple of the sine wave period, $1/f_0$ (Fig.1). The transmitting and receiving process is repeated $P$ times. At the $p$-th transmitting and receiving cycle, the transmitting signal corresponding to the $j$-th ($j$ = 0, 1, 2, ... , $N_T$-1) transmitter at $\boldsymbol{x}_{T\,j}$ and the waveform detected by the $i$-th ($i$ = 0, 1, 2, ... , $N_R$-1) receiver at $\boldsymbol{x}_{R\,i}$ are denoted by $u_j^{(p)}(t)$ and $r_i^{(p)}(t)$, respectively. The origins ($t$ = 0) of these functions are fixed at the starting positions of each transmitting pulse.

The transmitted pulse from the $j$-th transmitter at the $p$-th cycle is written as

$$u_j^{(p)}(t) = \begin{cases} \sum_{k=0}^{N_T-1} w_{(j\oplus p)k} \cdot f(t - k \cdot Dt) \cdots 0 \le t \le N_T Dt \\ 0 \qquad\qquad\qquad\qquad \cdots \mathrm{t} < 0,\ t > N_T Dt \end{cases} \quad (1)$$

where

$$f(t) = \begin{cases} \exp(j2pf_0 t) & 0 \le t \le Dt \\ 0 & t < 0,\ t > Dt \end{cases} \quad (2)$$

is a single sinusoidal pulse of frequency $f_0$, $w_{nm}$ denotes the ($n$, $m$) component of $N_T \times N_T$ Hadamard matrix, and $\oplus$ expresses the dyadic sum, that is, the modulo 2 addition for every corresponding bit of binary numbers. To simplify the equation, the column and row numbers are indexed from 0 to $N$-1.

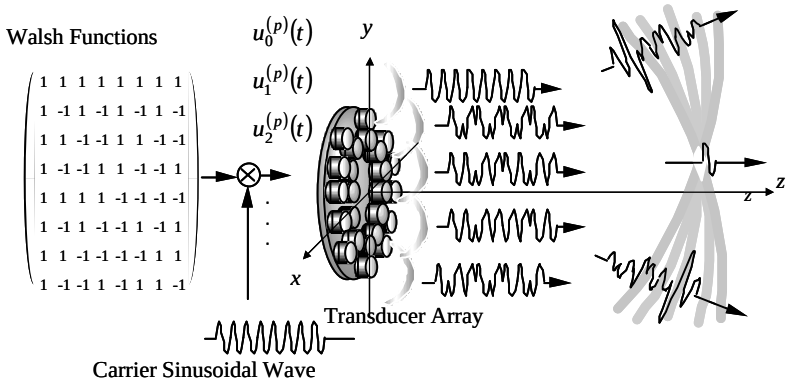


Fig. 1 Schematic drawing of the coded wavefront generated by Walsh function modulated pulses.

In a general form, the output, s($x$), of the focusing system for position $x$ is calculated as the sum of correlations between the received and expected echo functions for a single point target located at $x$. Thus, the output, s($x$), is calculated as

$$s(\boldsymbol{x}) = \left| \sum_p \int \sum_i r_i^{(p)} \left( t + \frac{|\boldsymbol{x} - \boldsymbol{x}_{R_i}|}{c} \right) \sum_j u_j^{(p)} \left( t - \frac{|\boldsymbol{x} - \boldsymbol{x}_{T_j}|}{c} \right)^* dt \right|^2 \quad (3)$$

This operation is regarded as a delay and sum operation followed by a matched filter-bank, where the filters are matched to the waveforms returned from each focus positions, *x*. The schematic diagram of the operation when the focus positions are in the paraxial region of the array is illustrated in Fig. 2.

Note that the operation is applied to the recorded echo waveforms and no direct transmitting beam forming is used. The transmitting beams as well as the receiving ones are synthesized using the echo waveforms. Dynamic focusing for the transmitting beams is possible with this method. This is an advantage of the method over the conventional beam forming method.

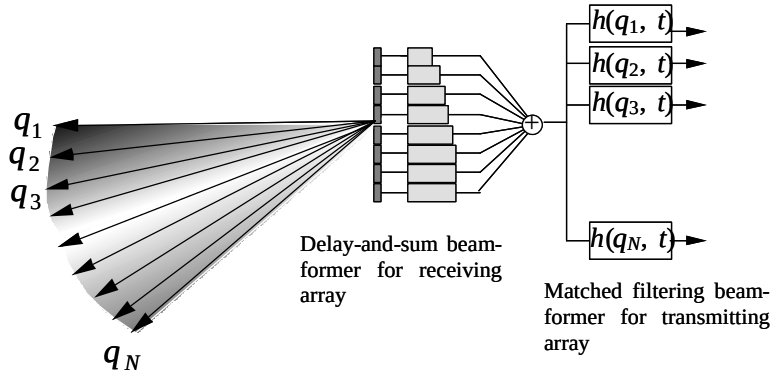


Fig. 2 Schematic diagram of beam forming.

## 3. Fabrication of 2D Array

### 3.1 Requirement of 2D Array Transducer

The beam profile of each element is an important design factor for 2D arrays. For synthetic aperture beam forming, a wide beam profile is preferred for a large region-of-interest (ROI) space. Beam width increases with decreasing element size. However, the echo sound intensity decreases for small elements. There is a trade-off between the beam profile and the echo signal level. It was determined that each element size was 1 mm × 1 mm, from echo signal level measurements by a standard ultrasonic phantom (ATS Lab. Model 539) and beam profile measurements.

Manufacturing a 2D array remains a technological challenge because of the very large number of elements with small lateral dimensions. We developed and set up a production process to manufacture fully connected $Pb(Zr_xTi_{1-x})O_3$ (PZT) 2D arrays. This process does not affect the acoustical behavior of each element and the connection of all of the elements is performed in a single operation. In addition, for the acoustical design, a specific backing and matching layers structure have been implemented to reduce crosstalk and to increase the acceptance angle.

### 3.2 PZT 40 × 40 Array Transducer

A 40 × 40 array of PZT elements was fabricated with a conventional dice-and-fill process. The array size was 40 mm × 40 mm. Since each element is relatively large (1 mm × 1 mm), the center frequency was selected to be 2 MHz in order to expand the ultrasonic beam. Figure 3(a) shows the structure of the PZT array transducer[7]. Signal lines were picked up by printed circuit boards (PCBs) through the backing layer. The PZT ceramics on the backing layer was diced-and-filled and then a silver film was deposited on top of the PZT ceramics to serve as a ground plane. After that, we place dual matching layers. A close up of the PZT 2D transducer is shown in Fig. 3(b). The area bound by the white rectangle denotes one channel. Each 1 mm × 1 mm element was subdiced into halves to achieve the desired aspect ratio.

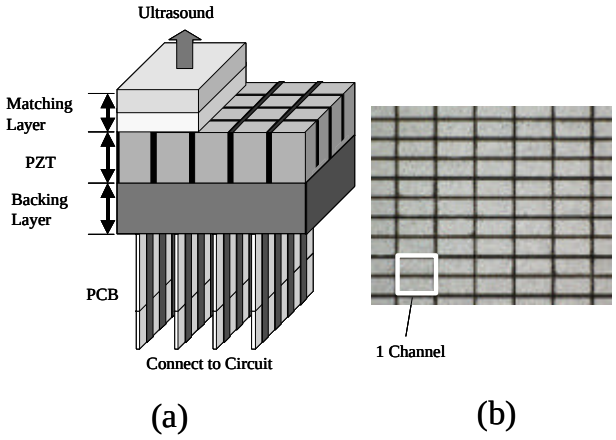


Fig. 3 (a) Schematic of a PZT 2D element array. (b) Close up of a diced PZT 2D array fabricated with a conventional dice-and-fill process. The area bound by the white rectangle denotes one channel. The diced cerfs are visible.

The center frequency was 2.1 MHz. The averaged -6 dB fractional bandwidth was 59.1%. The averaged sensitivity was -57.1 dBμV (echo level of alminum block, at a distance of 20 mm in water, with UTA-4 pulser and receiver) and the sensitivity variance was approximately 10 dB. Only 1.8% of the transducers among the 1600 elements were found to have a sensitivity less than -65 dBμV (expected value based on a preparatory experiment). The 40 × 40 element array was made using a plate of PZT ceramics, therefore each element was accurately positioned.

A sparse 2D array was fabricated by choosing 128 elements (Tx) and 128 elements (Rx) from 1600 elements. The elements were arranged to approximate a coaxial circular array. This geometry was adopted because such curvilinear arrays were experientially found to produce a better beam-pattern than periodic ones.

## 4. Experimental System

The experimental imaging system[8)] has been constructed as shown in Fig. 4. The system is composed of the developed 2D array transducer, peripheral electronic circuits that interface the array and front-end system, and personal computers (PCs) for the controller and data acquisition system, which provide computing power for image formation and display.

Transmitting signals were generated by digital pattern signals according to the Walsh functions. For the 32 transmitters, electrical pulses modulated by Walsh functions of 32 bits in length were used. The clock period, $\Delta t$ , was selected to be $2/f_0$, thus the duration time of the transmitted pulses was $32 \times 2/f_0$ =32 μs. The high-voltage signals were applied to the PZT elements with linear amplifiers (+/- 70 V). Receiving radio frequency (RF) signals were amplified by low-noise preamplifiers and digitized by 12 bit analog-to-digital (AD) converters (maximum sampling rate is 40 MHz). The digital data were transmitted to the PC with a high-speed low voltage differential signaling (LVDS) interface and a peripheral component interconnect (PCI) bus.

The maximum numbers of transmission and receiving channels of the data acquisition system are 64 and 128, respectively. A data acquisition system including 64 bits digital pattern generator and a 32-channel analog to digital converter (ADC) was attached to the developed transducer array.

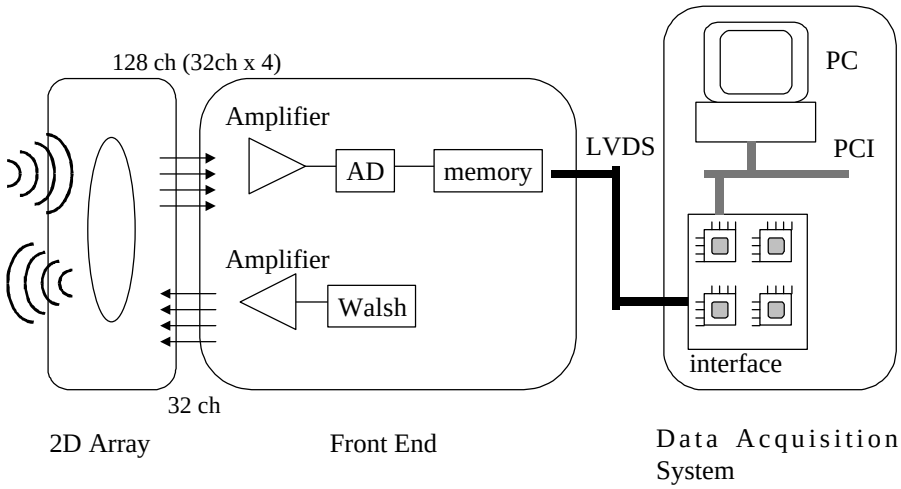


Fig. 4 Schematic drawing of the evaluation system using a coded wavefront.

## 5. Results and Discussion

To demonstrate the performance of the array, we first outline an experimental imaging conducted using the evaluation system. The experiments were carried out on the standard ultrasonic phantom (ATS Lab.: strings targets, cyst targets, attenuation coefficient of 0.5dB/ MHz/cm in Fig. 5) using the PZT 40 × 40 element array. Figure 6 shows a 3D view of the phantom with 32 transmissions. The imaged region is 70 × 70 × 70 $mm^3$. The structure of the strings can be recognized to be similar in brightness to conventional B-mode images.

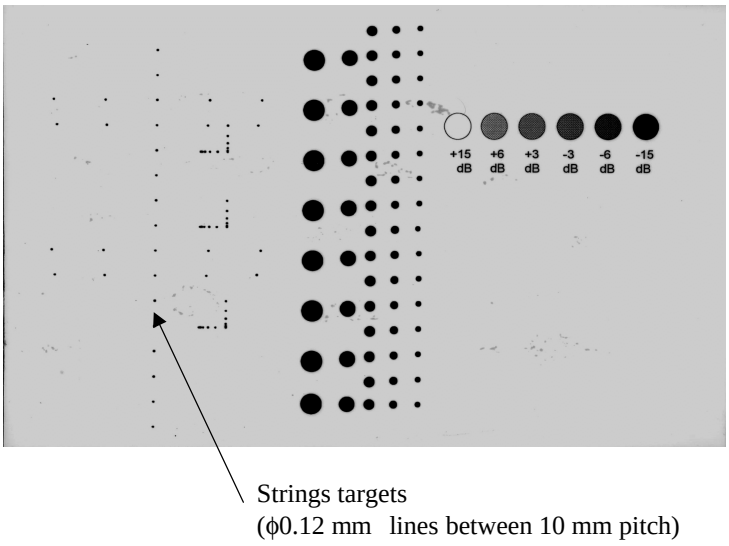


Fig. 5 Standard Ultrasonc phantom (ATS Lab.: Strings targets, cyst targets, attenuation coefficient of 0.5dB/ MHz/cm).

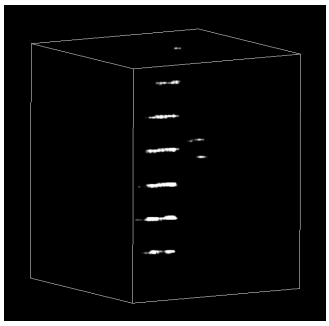

Fig. 6 3D view of the string targets. Imaged region is 70 × 70 × 70 $mm^3$.

Figure 7 shows the geometry of the experimental image planes. A B-mode image of string targets is shown in Fig.8(a). The image plane, which intersects the strings, is indicated as plane "B" in Fig. 7. An ultrasound convex-scanner, HS-3000 from Honda Electronics Co., LTD., was used. Fig. 8(b) shows a 3D image which was obtained by our system and projected onto plane "B". Another B-mode image and a projected 3D image of the same string targets according to plane "A" are shown in Fig.9(a) and 9(b), respectively. Note that two images, Fig.8(b) and 9(b) are the projected images of the same 3D image. The structure of the strings can be recognized in these images. From the 3D images, the directional and range resolution limits were evaluated as 1.4 degrees and 1 mm, respectively.

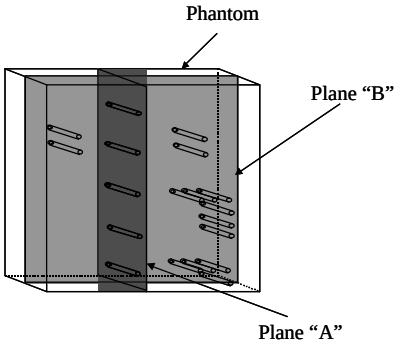


Fig. 7 Geometry of experimental image planes.

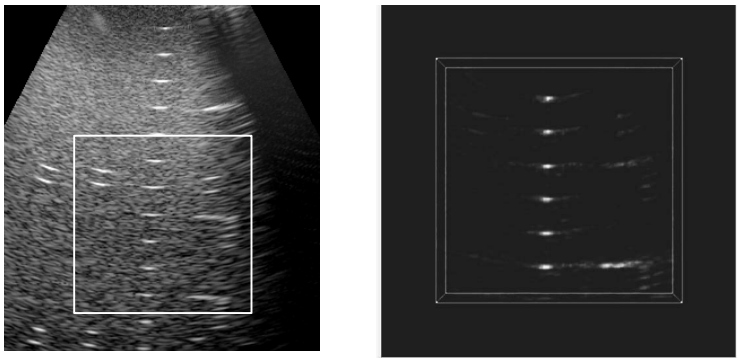

(a) (b)

Fig. 8 Images of the string targets. a): B-mode image in the plane "B" obtained by a convex scanner, b): 3D image projected to plane "B" obtained by the 3D system, the imaged region corresponds to a white square in a).

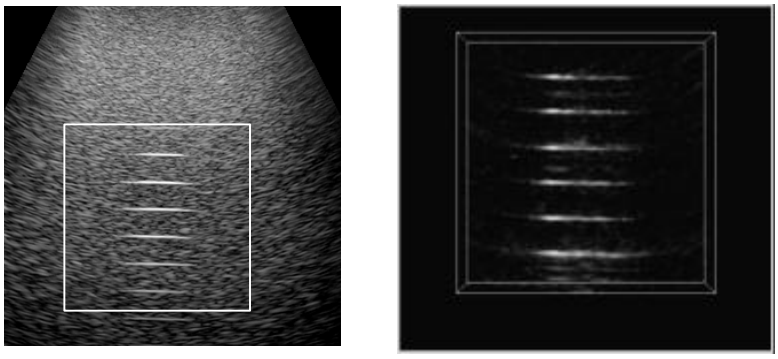

(a) (b)

Fig. 9 Images of the string targets. a): B mode image in the plane “A” obtained by a convex scanner, b): 3D image projected to plane “A” obtained by the 3D system of the string phantom.

Although the ability of the developed system to obtain 3D images of phantoms with very few transmission repetitions has been demonstrated, the quality of the images was insufficient for medical diagnostics. This is mainly because of the small number of active array elements and the properties of the modulating codes. We expect that a sufficient number of array elements and an image reconstructing operator which enhances the image quality[9, 10] will enable us to realize the diagnostic imaging system which operates on the proposed principle. We are investigating the required number of elements and a suitable imaging operator by means of computer simulations.

As a result of the experiment, the feasibility of the coded wavefront method for medical diagnostic 3D scanners was indicated using the developed 2D array. The PZT 40 × 40 element array is an excellent transducer with regard to positioning accuracy. Furthermore, it is necessary to have a wide aperture for the PZT 40 × 40 element array for abdominal diagnosis.

Although the manufacturing process for such large aperture 2D arrays is effective, it is difficult to realize a high yield ratio with the required accuracy. The defect ratio of the production process increases with an increase in the aperture size. We are going to develop a combined small-aperture PZT transmitter array and large aperture piezoelectric polymer P(VDF-TrFE) receiver array to solve this problem. A relatively small aperture PZT array using the developed process is quite useful because of the high stability of the properties of each element and its reasonable cost. The combined PZT / P(VDF-TrFE) array becomes possible while maintaining low cost and high efficiency in the bandwidth.

## 6. Conclusions

We have developed an experimental 2D array for a high-speed 3D imaging system. The size of the PZT 40 × 40 element array was 40 mm × 40 mm (each element is 1 mm × 1 mm, 2 MHz). Using this array, 3D images were successfully obtained for the standard ultrasound phantom with very few transmission repetitions, with 64 transmitters, 128 receivers and 32 transmissions. It is shown that the coded wavefront method is applicable in medical diagnosis.

## Acknowledgement

This research has been partially supported by grants from the New Energy and Industrial Technology Development Organization (NEDO) of Japan.

## References

1) S. W. Smith, H. G. Pavy and O. T. von Ramm: IEEE Trans. Ultrason. Ferroelectr. Freq. Control **38** (1994) 100.

2) S. W. Smith, H. G. Trahey and O. T. von Ramm: Ultrason. Imag. **14** (1992) 213.

3) E. D. Light, R. E. Davidsen, J. O. Fierng, T. A. Hruschka and S. W. Smith: Ultrason. Imag. **20** (1998) 235.

4) Y.Tamura and T. Akatsuka, Acoustical Imaging, **20**, (1993) 737.

5) G. R. Lockwood, R. Talman and S. S. Brunke, IEEE Transactions on UFFC, (1998) 45.

6) C. Ishihara, T. Aoki, N. Ishii, S. Hisamoto, H Yuasa and Y. Tamura, Acoustical Imaging **21** (1994) 765.

7) N. Okada, M. Sato, C. Ishihara, N. Ishii, T. Aoki, T. Hisamoto, H. Yanagida and Y. Tamura, Jpn. J. Appl. Phys., **42** (2003) in printing.

8) Y. Tamura, C. Ishihara, N. Okada, N. Ishii, M. Sato, T. Aoki, T. Hisamoto and H. Yanagida, *Proc. IEEE Int. Ultrasound, Munich,* (2002) 1661.

9) Y. Tamura, M. Takahashi and T. Akatsuka, Acoustical Imaging, **18** (1991) 481.

10) J. Shen and E. S. Ebbini, IEEE Transactions on UFFC, **43** (1996) 131.